Projected changes of surface winds over the Antarctic continental margin

Julia Neme[1], Matthew H. England[2], and Andrew McC. Hogg[3]

[1]UNSW Australia
[2]University of New South Wales
[3]Australian National University

November 23, 2022

Abstract

Surface winds around the Antarctic continent control coupled ocean-ice processes that influence the climate system, including bottom water production, heat transport onto the continental shelf and sea ice coverage. Few studies have examined projected changes in these winds, even though it would aid in the interpretation and understanding of the ocean's response to climate change. In this work we examine historical changes in the near-Antarctic surface winds using Coupled Model Intercomparison Project Phase 6 models and reanalysis data, and quantify projected changes to the end of the 21st Century. These changes include a significant reduction in both the easterly and meridional wind components, which under the high emission scenario amounts to 23% and 7% respectively, most of which occurs during the summer season. The projected weakening of surface winds are coherent with a trend towards a positive Southern Annular Mode and a reduction of the pole-to-coast meridional pressure gradient.

Projected changes of surface winds over the Antarctic continental margin

Julia Neme [1,2], Matthew H. England [1], Andrew McC. Hogg [3]

[1]Australian Centre for Excellence in Antarctic Science, University of New South Wales, Sydney, Australia.
[2]Climate Change Research Centre and ARC Centre of Excellence for Climate Extremes, University of New South Wales, Sydney, Australia.
[3]Research School of Earth Science and ARC Centre of Excellence for Climate Extremes, Australian National University, Canberra, Australia.

Key Points:

- Coupled Model Intercomparison Project Phase 6 models show a weakening of the near Antarctic surface winds during the period 1979-2015.
- Future projections in CMIP6 models show that the weakening trend continues until the end of the 21st Century.
- Weakened winds are associated with a more positive Southern Annular Mode and a reduction in the pole-to-coast meridional pressure gradient.

Corresponding author: Julia Neme, `j.neme@unsw.edu.au`

Abstract

Surface winds around the Antarctic continent control coupled ocean-ice processes that influence the climate system, including bottom water production, heat transport onto the continental shelf and sea ice coverage. Few studies have examined projected changes in these winds, even though it would aid in the interpretation and understanding of the ocean's response to climate change. In this work we examine historical changes in the near-Antarctic surface winds using Coupled Model Intercomparison Project Phase 6 models and reanalysis data, and quantify projected changes to the end of the 21st Century. These changes include a significant reduction in both the easterly and meridional wind components, which under the high emission scenario amounts to 23% and 7% respectively, most of which occurs during the summer season. The projected weakening of surface winds are coherent with a trend towards a positive Southern Annular Mode and a reduction of the pole-to-coast meridional pressure gradient.

Plain Language Summary

Surface winds over the ocean around the Antarctic continent influence several aspects of the oceanic circulation and sea ice in the region that become relevant in the context of climate change. For example, Antarctic coastal surface winds have been found to drive the warming experienced in some regions that subsequently triggers increased ice shelf melt. However, there is little understanding regarding how this wind regime is expected to change in the future, with most research focusing on the mid-latitude westerlies. In this work, we use Coupled Model Intercomparison Project Phase 6 models to quantify projected changes in these winds to the end of the 21st Century, hoping that it will aid in the interpretation of the ocean's response to climate change. We find a significant weakening of 23% for the easterly wind component and 7% for the meridional wind component. This weakening can be partly explained by a large scale pattern of change in sea level pressure that reflects in an increase of the atmospheric mode of variability known as the Southern Annular Mode, and a decrease of the pole-to-coast surface pressure gradient.

1 Introduction

Around much of the Antarctic continental margin there is a narrow band of easterly (westward flowing) surface winds that play a key role in controlling polar ocean circulation. In spite of their small meridional extent compared to other dominant features of the Southern Hemisphere atmospheric circulation, such as the more well-known subpolar westerlies, the easterlies influence processes critical to the ocean-ice response to climate change. The ocean processes on the Antarctic margin that are sensitive to changes in these winds include bottom water production (Stewart & Thompson, 2012, 2013; Wang et al., 2012), cross-shelf transport (Spence et al., 2014; A. F. Thompson et al., 2014) and sea-ice formation, melt and drift (Holland et al., 2019; Holland & Kwok, 2012). Despite their relevance, current and projected changes to the easterly wind regime have not been widely studied, with much more research devoted to understanding changes and impacts in the midlatitude westerly wind belt (Goyal, Sen Gupta, et al., 2021; Arblaster & Meehl, 2006).

The term "polar easterlies" for the circumpolar wind belt around the Antarctic continent, derived in analogy to the midlatitude westerlies, does not provide the most accurate description of this wind regime. The easterlies are subject to a strong topographic steering by the Antarctic continent and tend to be oriented in the direction of the coastline, which presents significant deviations from a purely zonal orientation (see Figure S1). Historically, the easterlies have been supposed to be partly driven by geostrophic adjustment via the Coriolis force in response to the katabatic wind regime, which is in turn forced by strong radiative cooling over the continent, as well as blocking effects due to the elevated terrain (Parish & Bromwich, 2007; Parish & Cassano, 2003; Van den Broeke & Van Lipzig, 2003; Davis & McNider, 1997; Parish & Bromwich, 1987). However, the katabatic wind regime is confined to a shallow surface layer and doesn't extend far from the coastline, which is why more recent work proposes that the easterlies are a balanced flow resulting from the Antarctic's orography and moderated by a potential vorticity anomaly atop of the plateau that is generated by radiative cooling (Fulton et al., 2017).

The polar wind regime influences a number of ocean-ice processes at the Antarctic margin that are critical for determining future rates of climate change and sea level rise. For example, the along-shore orientation of these winds induces an Ekman transport towards the continent that elevates coastal sea level, and their strength influences the cross-shore meridional density gradient, both processes that are responsible for sustaining the Antarctic Slope Current (ASC) and the Antarctic Slope Front (ASF) (Huneke et al., 2021; A. F. Thompson et al., 2018; Naveira Garabato et al., 2019; Mathiot et al., 2011). The ASC and ASF almost completely surround the Antarctic continent and act as a dynamical barrier to the exchange of heat and properties between the continental shelf and the deeper ocean (A. F. Thompson et al., 2018; Jacobs, 1991). Perturbations of the coastal easterlies thus have the ability to modify the cross-shelf exchange and are therefore one of the key factors that set the temperature anomalies responsible for warming of the continental shelf, thereby controlling basal melting of ice shelves (Holland et al., 2019; Spence et al., 2017, 2014). The abyssal meridional overturning circulation (MOC) that originates at the Antarctic margin, and even the Antarctic Circumpolar Current (ACC), have been suggested to be sensitive to the easterly winds (Zika et al., 2013; Stewart & Thompson, 2012). Finally, the local winds play a dominant role in sea-ice formation and advection (e.g. Kwok et al., 2017; Haumann et al., 2016; Holland & Kwok, 2012) as well as in the formation, extent and duration of polynyas (Mathiot et al., 2010; R. A. Massom et al., 1998; Bromwich & Kurtz, 1984).

One of the most well-known changes in the Southern Ocean's surface wind fields is the strengthening trend and poleward shift of the westerlies associated with both increased greenhouse gas emissions and stratospheric ozone depletion (e.g. Goyal, Sen Gupta, et al., 2021; Bracegirdle et al., 2008; Marshall, 2003). There are multiple studies examining the ocean's response to the trend in the Southern Hemisphere westerlies, including their impact on the meridional overturning, carbon and heat uptake, and water mass formation (e.g. Waugh et al., 2013; Sen Gupta & England, 2006; Oke & England, 2004; Hall & Visbeck, 2002; Toggweiler & Samuels, 1995). In comparison, there are very few studies that focus on historical and projected changes of the polar easterlies and their impact on the ocean circulation. Hazel and Stewart (2019) quantify trends in surface wind stress along the circumpolar 1000m isobath using different reanalysis products for the period 1979 to 2014 and find that there has been a substantial increase in their seasonality that results in an overall increase in their strength. However, the sparcity of observations in the region impairs the evaluation of reanalysis products in the region, particularly in relation to the reliability of its trends (Dong et al., 2020; Bracegirdle & Marshall, 2012). Regarding projected changes, using Coupled Model Intercomparison Project Phase 3 (CMIP3) models, Bracegirdle et al. (2008) find that the coastal easterlies are projected to weaken over the 21st Century in response to the poleward migration of the westerlies.

The aim of this study is to assess projected changes in CMIP6 models of the circumpolar wind belt around the Antarctic margin, commonly known as the polar easterlies, addressing the gap in research regarding future trends for polar surface wind regime. We also examine CMIP6 models during the historical period relative to four different reanalysis products. Given the importance of the easterlies for setting the Antarctic margin's circulation andh hence global sea level, characterizing projected changes will improve our understanding and interpretation of the ocean's response to climate change in CMIP6 models.

2 Data and Methods

This study analyses yearly-averaged and seasonal surface winds at 10m elevation and sea level pressure (SLP) from CMIP6 archives and four different reanalysis products over the ocean surrounding the Antarctic continent. We compare CMIP6 model output with reanalysis data for the historical period and assess future projected changes until the end of the 21st Century for the moderate and high emission scenarios, namely Shared Socio-economic Pathway 245 and 585 respectively (SSP245 and SSP585; (O'Neill et al., 2016)).

The CMIP6 models included in this study are listed in Table S1. We selected the first ensemble member for all models and remapped them onto a common 0.25° × 0.25° horizontal grid. The CMIP6 multi-model mean (MMM) was calculated by averaging all individual CMIP6 models using equal weights for each individual model. The reanalysis data sets selected for this study are the Climate Forecast System Reanalysis (CFSR, Saha et al. (2010)), ECMWF Interim Re-Analysis (ERA-Interim, Dee et al. (2011)), ERA-Interim's successor ERA5 (Hersbach et al., 2020) and the Japanese 55-year Reanalysis (JRA-55, Kobayashi et al. (2015)). None of these reanalysis products has been shown to be superior to the others in term of their performance in the Antarctic region, hence the decision to include them all (Dong et al., 2020; Gossart et al., 2019; Jones et al., 2016; Bracegirdle & Marshall, 2012). All reanalysis products were remapped onto the same 0.25° × 0.25° grid as CMIP6 models, and in analogy to the CMIP6 MMM, we calculate a multi-reanalysis mean. We define two analysis periods: the historical period, starting in 1979 and ending in 2015 and the future projections period starting in 2015 (when CMIP6 models constitute a projection) and ending in 2100 under SSP245 and SSP585 scenarios. For the calculation of trends and their significance, we use the publicly available implementation of the Mann-Kendall significance test developed by Moreno and Constantinou (2021).

The study region is defined as the oceanic domain from the Antarctic continent until a northern limit calculated from a combination of the minimum wind speed line and the 1000m isobath around the Antarctic Peninsula. The study region is defined in this way since the minimum wind speed line divides the wind field into mean westerlies to the north and mean easterlies to the south and includes regions of weak zonal winds in the Ross and Weddell Seas. However, because this line intersects the Antarctic Peninsula, we switch to using the 1000m isobath as our northern boundary in that region. We use the ERA-Interim wind field averaged over 1979 - 2015 to construct this boundary, after verifying that there is little variation in its position across both reanalysis products and models. The study region thus defined is shown in Figure 1.

3 Results

3.1 Historical Period

Surface winds around the Antarctic continent are stronger close to the coastline and decrease away from the coast, with regions adjacent to the steepest slopes around the continent displaying the strongest coastal winds, e.g. around East Antarctica (Figure 1). In the study region, CMIP6 MMM generally displays stronger winds than the multi-reanalysis mean, especially close to the coast in the western Ross Sea (Figure 1c). On the other hand, there are minimal differences in wind direction between CMIP6 MMM and the multi-reanalysis mean (Figure S2), which is likely because wind direction tends to be parallel to the coastline in this region, being subjected to a strong topographic control. There is also a significant component of the mean wind field that crosses SLP contours, highlighting the ageostrophic nature of the wind regime in this region.

The close agreement in the mean wind field between CMIP6 models and reanalysis products can also be seen in the averages as a function of longitude (Figure 2a,c).

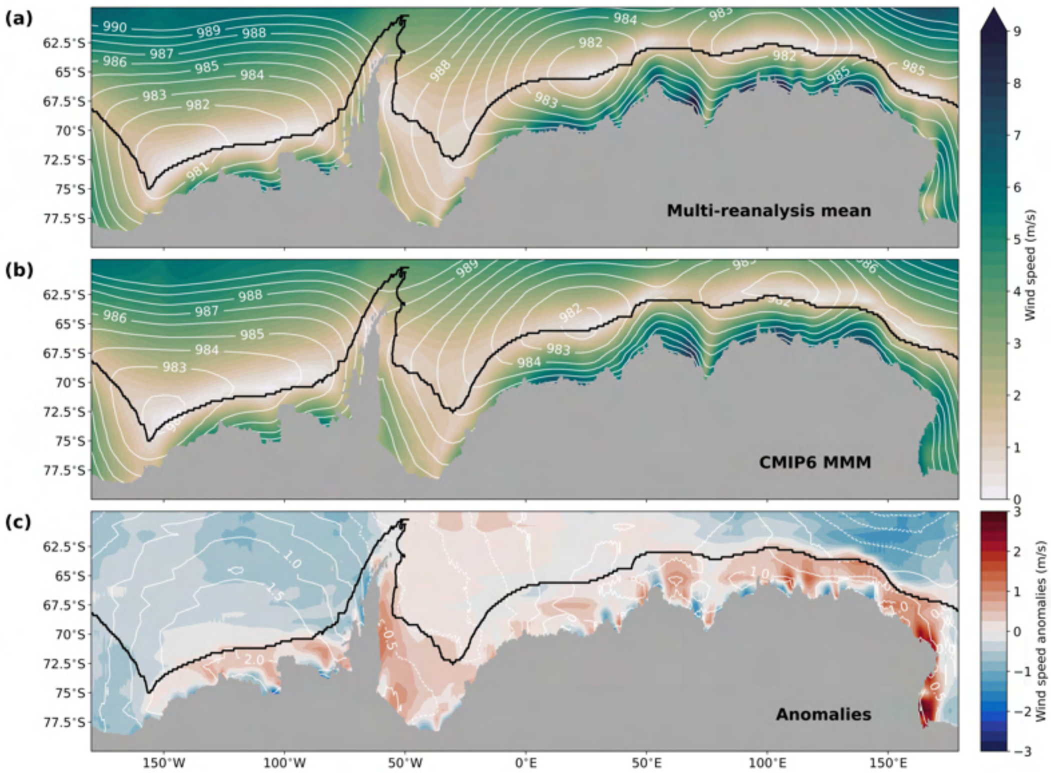

Figure 1. (a) Multi-reanalysis mean and (b) CMIP6 multi-model mean average wind speed (m/s) with contours of sea level pressure (hPa) for the period 1979 to 2015. (c) Wind speed and sea level pressure anomalies of CMIP6 multi-model mean with respect to the multi-reanalysis mean (a) - (b). The black contour in all panels marks the northern boundary of the study region. For wind vectors see Figure S1.

The zonal component shows the dominance of the easterly winds around the continent, except for around the tip of Antarctic Peninsula that extend north far enough to be embedded in the westerly wind regime, and the southwestern Weddell Sea and the Ross Sea where the orientation of the coastline favors a meridional flow. The meridional wind component shows the predominance of southerly winds flowing off the continent, except for a narrow band of onshore winds associated to the Amundsen Sea Low. The meridional wind component is subject to larger variations as a function of longitude than the zonal component, particularly over East Antarctica where changes of about 4m/s in speed occur over the span of a few degrees longitude (e.g. Figure 2c between 50°E and 100°E). This consistency between reanalysis products and models again indicates the strong influence of topography in setting the mean wind field direction.

Wind speed trends during the historical period are characterized by large local variations as well as differences in magnitude and sign of the trend between reanalysis products in both wind components, southerly and easterly (Figure 2b and c). There is little agreement in the pattern of trends shown across reanalysis products, as well as large small scale variability. In general, CMIP6 models show trends smaller in magnitude than the reanalysis products. One of the salient features of CMIP6 trends is the weakening trend in East Antarctica. The spatial patterns of easterly and southerly wind trends during the historical period displayed by CMIP6 MMM do not resemble those of the multi-reanalysis mean (Figures 2, S2, S3): CMIP6 MMM shows a clear pattern of weakening in our study region, significant around the Antarctic Peninsula and East Antarctica. This

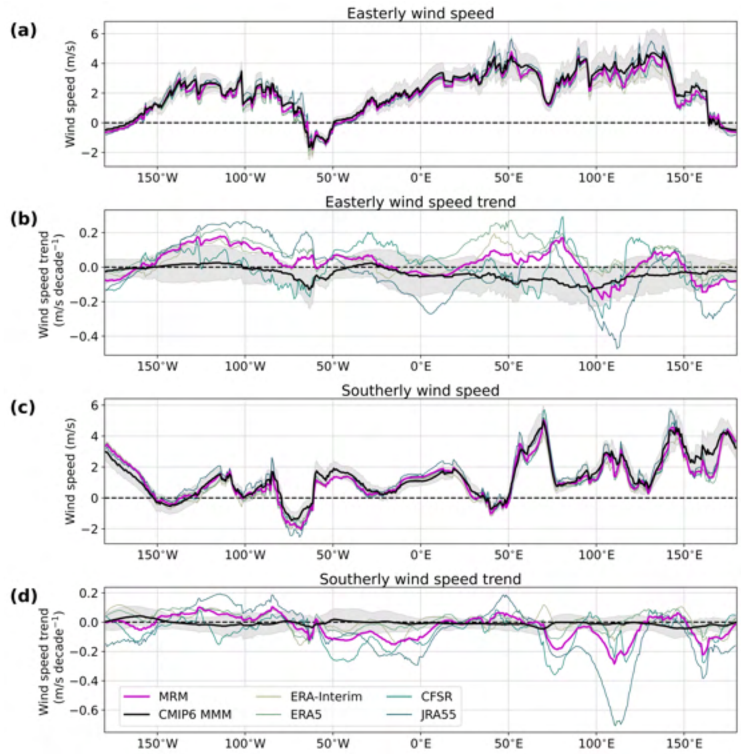

Figure 2. Mean (a) easterly and (c) southerly wind components (m/s) averaged as a function of longitude over the study region for the period 1979 to 2015. (b) Easterly and (d) southerly wind trends for the same period (m/s decade^{-1}) averaged as a function of longitude over the study region for the period 1979 to 2015. Included in all panels are CMIP6 multi-model mean and $\pm 1SD$ shading as well as the multi-reanalysis mean, ERA-Interim, ERA5, CFSR and JRA55.

is accompanied by a nearly zonally symmetric lowering of SLP around 65°S that reflects an increase in the SAM index that in turns projects onto an intensification and poleward migration of the westerly wind belt. This pattern is not apparent in the multi-reanalysis mean trends (Figure S3) because the reanalysis time period is strongly dominated by internal climate variability (Goyal, Jucker, Sen Gupta, & England, 2021). However, observed trends in the SAM index have been stronger in the late 20th Century for the summer season (December to February), subsequently weakening when entering the 21st Century due to stratospheric ozone recovery (Fogt & Marshall, 2020; Fogt et al., 2009). Therefore, we calculate trends for the summer season for the period 1979 to 2000, and corroborate that in this case, the multi-reanalysis mean does show a pattern related to the trend in the SAM index that weakens the easterly winds in some areas of our study region (Figure S4). Moreover, during this time period, the multi-reanalysis mean shows a better agreement with CMIP6 MMM trends (Figure S5). Therefore, we infer that on interannual time scales during the full historical period, 1979 to 2015, internal climate variability is dominating the multi-reanalysis mean trends, whereas the larger number of models included in the CMIP6 MMM effectively averages out any internal variability, thus highlighting the forced signal in that model ensemble set.

3.2 Future projections

Projected trends for the SSP585 scenario during the period 2015 to 2100 indicate a circumpolar weakening of the easterly wind component (Figure 3a). Scenario SSP245 shows similar patterns albeit with weaker trends (Figure S6). Similar to the historical period, the weakening trend within our study region is accompanied by a zonally symmetric lowering of sea level pressure indicative of a trend towards the high-index polarity of the SAM and the poleward migration of the westerlies. The poleward migration of the westerlies also inhibits the meridional wind component in the Antarctic Peninsula (Figure 3b), and more generally around East Antarctica. The trend towards a positive SAM index is also linked to a deepening of the Amundsen Sea Low (Clem et al., 2017, 2016), which drives a strengthening of the offshore winds in the Ross Sea and an adjacent weakening in the Amundsen-Bellinghausen Seas (Figure 3b).

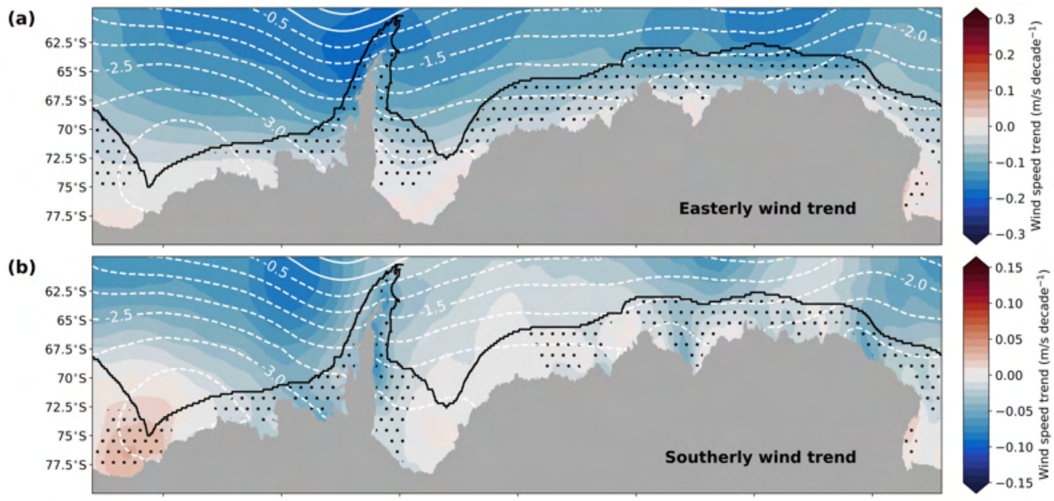

Figure 3. CMIP6 multi-model mean trends for a) easterly and b) southerly wind for emission scenario SSP585 during the period 2015 to 2100, with statistically significant trends with $p < 0.05$ hatched only for the study region. Pink contours show the difference in SLP of the last ten years (2090 to 2099) relative to the first ten years (2015 to 2025) and the black contour marks the northern limit of our study region.

We next perform an average over the entire study region to quantify the large scale changes in the polar winds (Figure 4). This circumpolar average allows us to study broad scale changes without focusing on the local variations observed in individual models and reanalyses. During the historical period, peaks and troughs for both components of the wind are in phase among reanalysis products, indicating all products capture the overall year-to-year variations in circumpolar-averaged winds. In contrast in the CMIP6 models, the averaging of different models has a smoothing effect on the time series. None of the reanalysis product trends for the easterly wind component are significant at the 5% level, whereas for the southerly wind component CFSR, JRA55 and the multi-reanalysis mean display significant weakening trends (Figure 4, Table S2). Trends for the CMIP6 MMM are significant during the historical period, and future projections under both scenarios considered.

For the easterly wind component, CMIP6 MMM displays a significant weakening trend during the historical period of 0.41m/s century^{-1} ($p < 0.05$) (Figure 4b). However, due to the large intermodel spread, while 50% of the models display trends toward weakening easterlies, there are some models that display a strengthening trend. For the southerly component, CMIP6 MMM shows slight, significant weakening trend of 0.08m/s century^{-1}, but there is a larger number of models that display strengthening trend. No models display trends as large as those present in CFSR and JRA55. Future projections show that the weakening in both wind components extends until the end of the 21st Cen-

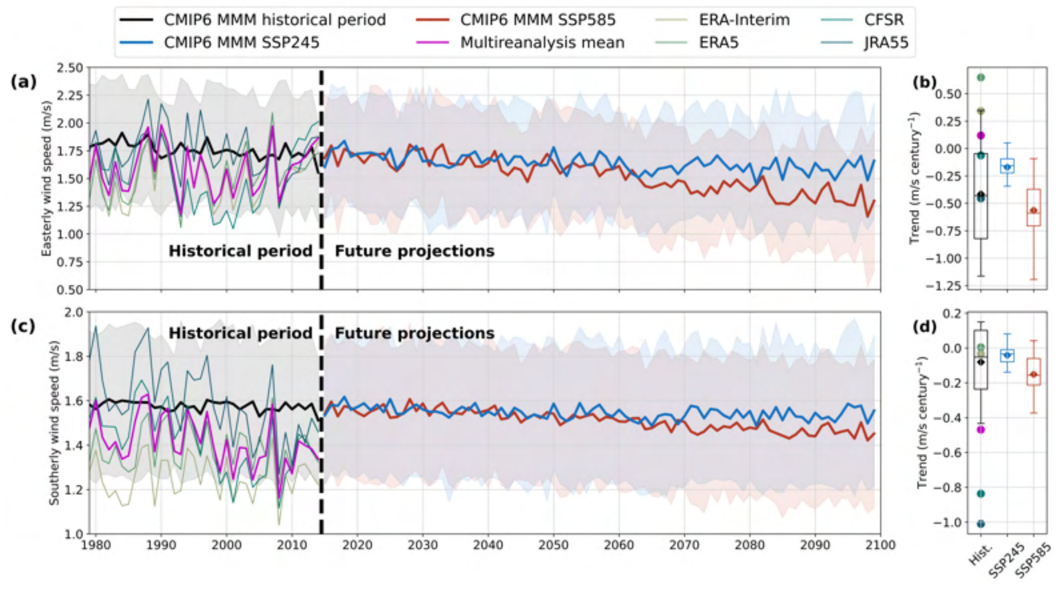

Figure 4. (a) Easterly and (c) southerly wind speed averaged over the study region for CMIP6 multi-model mean and $\pm 1SD$ shading, the multi-reanalysis mean, ERA-Interim, ERA5, CFSR and JRA55. Boxplot of (b) easterly and (d) southerly wind trends (m/s century^{-1}) for CMIP6 models for the historical period, SSP245 and SSP585. Dots mark trends in CMIP6 multi-model mean, multi-reanalysis mean, ERA-Interim, ERA5, CFSR and JRA55.

tury. Under the SSP245 scenario the trends are weaker compared with the historical period, while for the SSP585 scenario the CMIP6 MMM average trend increases to 0.56m/s century^{-1}. In both scenarios the intermodel range is reduced, and for SSP585 all models agree on a weakening trend. A similar behaviour is observed for the southerly component: namely for the SSP245 scenario, the trend is slightly lower than during the historical period, while the trend increases in SSP585. However for the southerly component, some models display trends of opposite sign towards strengthening of the southerlies in both scenarios. Given that trends in the position of the westerly wind belt in CMIP6 models have been found to be seasonally dependent (Goyal, Sen Gupta, et al., 2021), we repeat the above analysis separately for the summer (December to February) and winter (June to August) seasons (Figure S9, S9). We find that the largest weakening trends occur during the summer season, consistent with seasonal trends in westerly winds, with no significant changes during the winter season (for details see Tables S3, S4).

The observed spatial patterns of trends in the region occur in conjunction with a lowering of SLP, almost zonally symmetric in character, at around $65°S$ (Figure 3, S2, S3). This reduction in SLP projects onto a increasingly positive SAM index, as well as onto a reduced meridional SLP gradient between the pole and $65°S$. Both of these changes have a weakening effect on the near-Antarctic wind regime: in particular, the positive trend in the SAM index implies a poleward migration of the westerlies that extends sufficiently far southwards to impact our study region, and the reduced pole-to-coast meridional pressure gradient weakens the easterly wind component via a geostrophic adjustment. This relationship is apparent in the correlations between the SAM index (calculated following Gong and Wang (1999) as the pressure difference between 45°S and 65°S) and the time series in Figure 4; as well as in the correlations with a katabatic wind index (calculated following Hazel and Stewart (2019) as the pressure difference between 85°S and 65°S: Figure S7). For the CMIP6 MMM, under the SSP585 scenario, the correlations of the easterly wind component with the SAM and katabatic wind indices are as high as -0.93 and 0.93 respectively.

4 Summary and Discussion

The Southern Ocean's circulation close to the Antarctic margin is a key component of the Earth's climate system, regulating heat, atmospheric CO_2 concentration, ice melt and sea level (Frölicher et al., 2015; Golledge et al., 2015; Mikaloff Fletcher et al., 2006). There is thus a growing interest in constraining projected changes in the atmospheric circulation in this region. Despite their relevance for the Antarctic margin ocean circulation, the polar wind belt remains one of the most understudied features of the region, with few studies documenting current and future changes (Hazel & Stewart, 2019; Bracegirdle et al., 2008). Our study examines the near-Antarctic wind field and its projected changes in CMIP6 models, comparing the historical period against four different reanalysis products: ERA-Interim, ERA5, CFSR and JRA55. We find a good agreement between the mean wind and sea level pressure fields of CMIP6 models and reanalysis products during the historical period, suggesting that CMIP6 models are capable of simulating the broad features apparent in reanalyses (Figures 2a, c, S1). We attribute this consistency to the strong topographic steering of winds by the Antarctic continent and orography (e.g. as noted by Goyal, Jucker, Sen Gupta, and England (2021) for the Amundsen Sea Low). However this agreement in mean wind fields does not translate to an agreement in the spatial pattern of wind speed trends. The trends for the easterly and southerly wind components display significant small scale variability as well as large differences across reanalysis products and models (Figure 2). However, it should be noted that reanalysis products are poorly constrained in the study region and some studies have reported spurious trends at small spatial scales in the Antarctic region (Dong et al., 2020; Huai et al., 2019; Bracegirdle & Marshall, 2012; Wang et al., 2012). Furthermore, there are significant patterns of atmospheric variability in the Southern Ocean that act over time scales ranging from months to decades, such as the SAM (D. W. Thompson et al., 2011; D. W. Thompson & Solomon, 2002), ENSO (Meehl et al., 2019; Fogt & Bromwich, 2006; Turner, 2004), IPO (Purich et al., 2016; Meehl et al., 2013) and zonal wavenumber 3 (Goyal, Jucker, Sen Gupta, Hendon, & England, 2021; Raphael, 2007). These intrinsic modes can have a large impact on atmospheric circulation, confounding a comparison between observations and models. For example, prior to the year 2000, there have been strong observed trends towards a positive SAM index during the summer months (Fogt & Marshall, 2020; Fogt et al., 2009; D. W. Thompson & Solomon, 2002) which are apparent in the multi-reanalysis mean trends (Figure S4). However, trends of the yearly-averaged data during the entire historical period in the multi-reanalysis period are dominated by internal variability, which is, in contrast, averaged out in the CMIP6 MMM where the forced signal related to SAM changes is clearly visible (Figure S2).

On average, CMIP6 MMM shows that the easterly wind component is projected to weaken over the next century by 6% for SSP245 and 23% for SSP585 relative to the 2005-2015 mean. Most of this weakening occurs during the summer months (7% and 34% reduction for SSP245 and SSP585 scenarios respectively), with no significant changes during the winter season, meaning that there is an increase in the amplitude of the seasonal cycle (Figure S8, S9). As wind stress scales with wind speed squared, these large reductions will have significant impacts on the oceanic circulation in the region. For example, shoreward Ekman transport would be reduced substantially, leading to a decrease in coastal sea level that weakens coastal currents, increases in heat transport towards the continental shelf and potentially leads to substancial ice sheet melt. Projected changes of the southerly wind component are not as consistent as those of the easterly component, in that some CMIP6 individual models display trends of opposite sign (Figure 4d). Nonetheless, CMIP6 MMM shows a significant weakening trend for the southerlies of 2% and 7% in wind speed at the end of the 21st Century with respect to the 2005 - 2015 average. The southerly (offshore) component of the surface winds at the Antarctic margin plays an important role in Dense Shelf Water production via the opening of coastal polynyas, where strong air-sea interactions trigger large surface water mass transformation (Huot et al., 2021; Mathiot et al., 2010; R. Massom et al., 1998). Therefore, this significant projected reduction in the southerlies strength is likely to impact the rates of formation of Dense Shelf Waters around Antarctica.

There are important caveats to note regarding the data sets used in this study, mostly related to the reliability of trends depicted in reanalysis products and CMIP6 models. Lack of sufficient observations limits the evaluation of these trends, especially their spatial distributions, and their attribution to internal or forced variability. However, there is a robust relationship between meridional sea level pressure gradients and easterly wind speed averages over the study region. For most reanalysis products and CMIP6 individual models, there is a significant correlation between the strength of the easterlies and the SAM index, defined following Marshall (2003), as well as the pole-to-coast (katabatic) index, defined following the methodology of Hazel and Stewart (2019) (Figure S7). The relationships that can be inferred from these correlations are consistent with the notion that the poleward migration of the westerly wind belt inhibits the polar easterlies, and that a reduced pole-to-coast pressure gradient weakens the katabatic regime, which in turn translates into weaker easterlies. All but two CMIP6 individual models display significant high correlations between both components of the surface winds with the sea level pressure indices described above, indicating a robust large-scale pattern of change that continues until the end of the century.

Understanding current and projected changes in the Antarctic margin wind regime in CMIP6 models is vital for the interpretation and attribution of changes in the high-latitude ocean circulation. This study identifies the emergence of a large scale, significant weakening of this wind regime that can be attributed to the poleward migration and intensification of the subpolar westerlies, as well as a reduction in the pole-to-coast meridional sea level pressure gradient.

Acknowledgments

This work was supported by the Australian Research Council, including the ARC Centre of Excellence for Climate Extremes, ARC Australian Centre for Excellence in Antarctic Science and the Climate Change Research Centre of the University of New South Wales. All the analysis in this study was conducted at the NCI National Facility systems at the Australian National University, which is supported by the Australian Government. All data sets analyzed in this study are publicly available. CMIP6 model data can be obtained from the Earth Systems Grid Federation website `https://esgf-node.llnl.gov/projects/cmip6/`. ERA-Interim data set can be downloaded from `https://www.ecmwf.int/en/forecasts/datasets/reanalysis-datasets/era-interim`, ERA5 from `https://www.ecmwf.int/en/forecasts/datasets/reanalysis-datasets/era5`, CFSR from `https://climatedataguide.ucar.edu/climate-data/climate-forecast-system-reanalysis-cfsr` and JRA55 from `https://climatedataguide.ucar.edu/climate-data/jra-55`. The authors thank Josue M. Moreno and Navid C. Constatinou for developing and making available their python package for computing linear trends.

References

Arblaster, J. M., & Meehl, G. A. (2006). Contributions of external forcings to southern annular mode trends. *Journal of Climate*, *19*(12), 2896 - 2905. Retrieved from `https://journals.ametsoc.org/view/journals/clim/19/12/jcli3774.1.xml` doi: 10.1175/JCLI3774.1

Bracegirdle, T. J., Connolley, W. M., & Turner, J. (2008). Antarctic climate change over the twenty first century. *Journal of Geophysical Research: Atmospheres*, *113*(D3).

Bracegirdle, T. J., & Marshall, G. J. (2012). The reliability of antarctic tropospheric pressure and temperature in the latest global reanalyses. *Journal of Climate*, *25*(20), 7138–7146.

Bromwich, D. H., & Kurtz, D. D. (1984). Katabatic wind forcing of the terra nova bay polynya. *Journal of Geophysical Research: Oceans*, *89*(C3), 3561–3572.

Clem, K. R., Renwick, J. A., & McGregor, J. (2017). Large-scale forcing of the amundsen sea low and its influence on sea ice and west antarctic temperature. *Journal of Climate*, *30*(20), 8405–8424.

Clem, K. R., Renwick, J. A., McGregor, J., & Fogt, R. L. (2016). The relative influence of enso and sam on antarctic peninsula climate. *Journal of Geophysical Research: Atmospheres*, *121*(16), 9324–9341.

Davis, A., & McNider, R. (1997). The development of antarctic katabatic winds and implications for the coastal ocean. *Journal of the atmospheric sciences*, *54*(9), 1248–1261.

Dee, D. P., Uppala, S. M., Simmons, A., Berrisford, P., Poli, P., Kobayashi, S., ... others (2011). The era-interim reanalysis: Configuration and performance of the data assimilation system. *Quarterly Journal of the royal meteorological society*, *137*(656), 553–597.

Dong, X., Wang, Y., Hou, S., Ding, M., Yin, B., & Zhang, Y. (2020). Robustness of the recent global atmospheric reanalyses for antarctic near-surface wind speed climatology. *Journal of Climate*, *33*(10), 4027–4043.

Fogt, R. L., & Bromwich, D. H. (2006). Decadal variability of the enso teleconnection to the high-latitude south pacific governed by coupling with the southern annular mode. *Journal of Climate*, *19*(6), 979–997.

Fogt, R. L., & Marshall, G. J. (2020). The southern annular mode: variability, trends, and climate impacts across the southern hemisphere. *Wiley Interdisciplinary Reviews: Climate Change*, *11*(4), e652.

Fogt, R. L., Perlwitz, J., Monaghan, A. J., Bromwich, D. H., Jones, J. M., & Marshall, G. J. (2009). Historical sam variability. part ii: Twentieth-century variability and trends from reconstructions, observations, and the ipcc ar4 models. *Journal of Climate*, *22*(20), 5346–5365.

Frölicher, T. L., Sarmiento, J. L., Paynter, D. J., Dunne, J. P., Krasting, J. P., & Winton, M. (2015). Dominance of the southern ocean in anthropogenic carbon and heat uptake in cmip5 models. *Journal of Climate*, *28*(2), 862–886.

Fulton, S. R., Schubert, W. H., Chen, Z., & Ciesielski, P. E. (2017). A dynamical explanation of the topographically bound easterly low-level jet surrounding antarctica. *Journal of Geophysical Research: Atmospheres*, *122*(23), 12–635.

Golledge, N. R., Kowalewski, D. E., Naish, T. R., Levy, R. H., Fogwill, C. J., & Gasson, E. G. (2015). The multi-millennial antarctic commitment to future sea-level rise. *Nature*, *526*(7573), 421–425.

Gong, D., & Wang, S. (1999). Definition of antarctic oscillation index. *Geophysical research letters*, *26*(4), 459–462.

Gossart, A., Helsen, S., Lenaerts, J., Broucke, S. V., Van Lipzig, N., & Souverijns, N. (2019). An evaluation of surface climatology in state-of-the-art reanalyses over the antarctic ice sheet. *Journal of Climate*, *32*(20), 6899–6915.

Goyal, R., Jucker, M., Sen Gupta, A., & England, M. H. (2021). Generation of the amundsen sea low by antarctic orography. *Geophysical Research Letters*, *48*(4), e2020GL091487.

Goyal, R., Jucker, M., Sen Gupta, A., Hendon, H. H., & England, M. H. (2021). Zonal wave 3 pattern in the southern hemisphere generated by tropical convection. *Nature Geoscience*, *14*(10), 732–738.

Goyal, R., Sen Gupta, A., Jucker, M., & England, M. H. (2021). Historical and projected changes in the southern hemisphere surface westerlies. *Geophysical Research Letters*, *48*(4), e2020GL090849.

Hall, A., & Visbeck, M. (2002). Synchronous variability in the southern hemisphere atmosphere, sea ice, and ocean resulting from the annular mode. *Journal of Climate*, *15*(21), 3043–3057.

Haumann, F. A., Gruber, N., Münnich, M., Frenger, I., & Kern, S. (2016). Sea-ice transport driving southern ocean salinity and its recent trends. *Nature*, *537*(7618), 89–92.

Hazel, J. E., & Stewart, A. L. (2019). Are the near-antarctic easterly winds weakening in response to enhancement of the southern annular mode? *Journal of Climate*, *32*(6), 1895–1918.

Hersbach, H., Bell, B., Berrisford, P., Hirahara, S., Horányi, A., Muñoz-Sabater, J., ... others (2020). The era5 global reanalysis. *Quarterly Journal of the Royal Meteorological Society*, *146*(730), 1999–2049.

Holland, P. R., Bracegirdle, T. J., Dutrieux, P., Jenkins, A., & Steig, E. J. (2019). West antarctic ice loss influenced by internal climate variability and anthropogenic forcing. *Nature Geoscience*, *12*(9), 718–724.

Holland, P. R., & Kwok, R. (2012). Wind-driven trends in antarctic sea-ice drift. *Nature Geoscience*, *5*(12), 872–875.

Huai, B., Wang, Y., Ding, M., Zhang, J., & Dong, X. (2019). An assessment of recent global atmospheric reanalyses for antarctic near surface air temperature. *Atmospheric Research*, *226*, 181–191.

Huneke, W. G., Morrison, A. K., & Hogg, A. M. (2021). Spatial and subannual variability of the antarctic slope current in an eddying ocean-sea ice model. *Journal of Physical Oceanography*.

Huot, P.-V., Kittel, C., Fichefet, T., Jourdain, N. C., Sterlin, J., & Fettweis, X. (2021). Effects of the atmospheric forcing resolution on simulated sea ice and polynyas off adélie land, east antarctica. *Ocean Modelling*, *168*, 101901.

Jacobs, S. S. (1991). On the nature and significance of the antarctic slope front. *Marine Chemistry*, *35*(1-4), 9–24.

Jones, R., Renfrew, I., Orr, A., Webber, B., Holland, D., & Lazzara, M. (2016). Evaluation of four global reanalysis products using in situ observations in the amundsen sea embayment, antarctica. *Journal of Geophysical Research: Atmospheres*, *121*(11), 6240–6257.

Kobayashi, S., Ota, Y., Harada, Y., Ebita, A., Moriya, M., Onoda, H., ... others (2015). The jra-55 reanalysis: General specifications and basic characteristics. *Journal of the Meteorological Society of Japan. Ser. II*, *93*(1), 5–48.

Kwok, R., Pang, S. S., & Kacimi, S. (2017, 06). Sea ice drift in the Southern Ocean: Regional patterns, variability, and trends. *Elementa: Science of the Anthropocene*, *5*. Retrieved from `https://doi.org/10.1525/elementa.226` (32) doi: 10.1525/elementa.226

Marshall, G. J. (2003). Trends in the southern annular mode from observations and reanalyses. *Journal of climate*, *16*(24), 4134–4143.

Massom, R., Harris, P., Michael, K. J., & Potter, M. (1998). The distribution and formative processes of latent-heat polynyas in east antarctica. *Annals of Glaciology*, *27*, 420–426.

Massom, R. A., Harris, P., Michael, K. J., & Potter, M. (1998). The distribution and formative processes of latent-heat polynyas in east antarctica. *Annals of Glaciology*, *27*, 420–426. doi: 10.3189/1998AoG27-1-420-426

Mathiot, P., Barnier, B., Gallée, H., Molines, J. M., Le Sommer, J., Juza, M., & Penduff, T. (2010). Introducing katabatic winds in global era40 fields to simulate their impacts on the southern ocean and sea-ice. *Ocean Modelling*, *35*(3), 146–160.

Mathiot, P., Goosse, H., Fichefet, T., Barnier, B., & Gallée, H. (2011). Modelling the seasonal variability of the antarctic slope current. *Ocean Science*, *7*(4), 455–470.

Meehl, G. A., Arblaster, J. M., Chung, C. T., Holland, M. M., DuVivier, A., Thompson, L., ... Bitz, C. M. (2019). Sustained ocean changes contributed to sudden antarctic sea ice retreat in late 2016. *Nature Communications*, *10*(1), 1–9.

Meehl, G. A., Hu, A., Arblaster, J. M., Fasullo, J., & Trenberth, K. E. (2013). Externally forced and internally generated decadal climate variability associated with the interdecadal pacific oscillation. *Journal of Climate*, *26*(18), 7298–7310.

Mikaloff Fletcher, S. E., Gruber, N., Jacobson, A. R., Doney, S. C., Dutkiewicz, S., Gerber, M., ... others (2006). Inverse estimates of anthropogenic co2 uptake, transport, and storage by the ocean. *Global biogeochemical cycles*, *20*(2).

Moreno, J. M., & Constantinou, N. C. (2021, January). *josuemtzmo/xarrayMannKendall: Mann Kendall significance test implemented in xarray.* Zenodo. Retrieved from `https://doi.org/10.5281/zenodo.4458777` doi: 10.5281/zenodo.4458777

Naveira Garabato, A., Dotto, T., Hooley, J., Bacon, S., Tsamados, M., Ridout, A., ... others (2019). Phased response of the subpolar southern ocean to changes in circumpolar winds. *Geophysical Research Letters*, *46*(11), 6024–6033.

Oke, P. R., & England, M. H. (2004). Oceanic response to changes in the latitude of the southern hemisphere subpolar westerly winds. *Journal of Climate*, *17*(5), 1040–1054.

O'Neill, B. C., Tebaldi, C., Van Vuuren, D. P., Eyring, V., Friedlingstein, P., Hurtt, G., ... others (2016). The scenario model intercomparison project (scenariomip) for cmip6. *Geoscientific Model Development*, *9*(9), 3461–3482.

Parish, T. R., & Bromwich, D. H. (1987). The surface windfield over the antarctic ice sheets. *Nature*, *328*(6125), 51–54.

Parish, T. R., & Bromwich, D. H. (2007). Reexamination of the near-surface airflow over the antarctic continent and implications on atmospheric circulations at high southern latitudes. *Monthly Weather Review*, *135*(5), 1961–1973.

Parish, T. R., & Cassano, J. J. (2003). The role of katabatic winds on the antarctic surface wind regime. *Monthly Weather Review*, *131*(2), 317–333.

Purich, A., England, M. H., Cai, W., Chikamoto, Y., Timmermann, A., Fyfe, J. C., ... Arblaster, J. M. (2016). Tropical pacific sst drivers of recent antarctic sea ice trends. *Journal of Climate*, *29*(24), 8931–8948.

Raphael, M. N. (2007). The influence of atmospheric zonal wave three on antarctic sea ice variability. *Journal of Geophysical Research: Atmospheres*, *112*(D12).

Saha, S., Moorthi, S., Pan, H.-L., Wu, X., Wang, J., Nadiga, S., ... others (2010). The ncep climate forecast system reanalysis. *Bulletin of the American Meteorological Society*, *91*(8), 1015–1058.

Sen Gupta, A., & England, M. H. (2006). Coupled ocean–atmosphere–ice response to variations in the southern annular mode. *Journal of Climate*, *19*(18), 4457–4486.

Spence, P., Griffies, S. M., England, M. H., Hogg, A. M., Saenko, O. A., & Jourdain, N. C. (2014). Rapid subsurface warming and circulation changes of antarctic coastal waters by poleward shifting winds. *Geophysical Research Letters*, *41*(13), 4601–4610.

Spence, P., Holmes, R. M., Hogg, A. M., Griffies, S. M., Stewart, K. D., & England, M. H. (2017). Localized rapid warming of west antarctic subsurface waters by remote winds. *Nature Climate Change*, *7*(8), 595–603.

Stewart, A. L., & Thompson, A. F. (2012). Sensitivity of the ocean's deep overturning circulation to easterly antarctic winds. *Geophysical Research Letters*, *39*(18).

Stewart, A. L., & Thompson, A. F. (2013). Connecting antarctic cross-slope exchange with southern ocean overturning. *Journal of Physical Oceanography*, *43*(7), 1453–1471.

Thompson, A. F., Heywood, K. J., Schmidtko, S., & Stewart, A. L. (2014). Eddy transport as a key component of the antarctic overturning circulation. *Nature Geoscience*, *7*(12), 879–884.

Thompson, A. F., Stewart, A. L., Spence, P., & Heywood, K. J. (2018). The antarctic slope current in a changing climate. *Reviews of Geophysics*, *56*(4), 741–770.

Thompson, D. W., & Solomon, S. (2002). Interpretation of recent southern hemisphere climate change. *Science*, *296*(5569), 895–899.

Thompson, D. W., Solomon, S., Kushner, P. J., England, M. H., Grise, K. M., & Karoly, D. J. (2011). Signatures of the antarctic ozone hole in southern hemisphere surface climate change. *Nature geoscience*, *4*(11), 741–749.

Toggweiler, J., & Samuels, B. (1995). Effect of drake passage on the global thermohaline circulation. *Deep Sea Research Part I: Oceanographic Research Papers*, *42*(4), 477–500.

Turner, J. (2004). The el nino–southern oscillation and antarctica. *International Journal of Climatology: A Journal of the Royal Meteorological Society*, *24*(1), 1–31.

Van den Broeke, M., & Van Lipzig, N. (2003). Factors controlling the near-surface wind field in antarctica. *Monthly Weather Review*, *131*(4), 733–743.

Wang, Q., Danilov, S., Fahrbach, E., Schröter, J., & Jung, T. (2012). On the impact of wind forcing on the seasonal variability of weddell sea bottom water transport. *Geophysical Research Letters*, *39*(6).

Waugh, D. W., Primeau, F., DeVries, T., & Holzer, M. (2013). Recent changes in the ventilation of the southern oceans. *Science*, *339*(6119), 568-570. Retrieved from `https://www.science.org/doi/abs/10.1126/science.1225411` doi: 10.1126/science.1225411

Zika, J. D., Le Sommer, J., Dufour, C. O., Naveira-Garabato, A., & Blaker, A. (2013). Acceleration of the antarctic circumpolar current by wind stress along the coast of antarctica. *Journal of physical oceanography*, *43*(12), 2772–2784.

Supporting Information for "Projected changes of surface winds over the Antarctic continental margin"

Julia Neme [1,2], Matthew H. England [2], Andrew McC. Hogg [3]

[1]Climate Change Research Centre and ARC Centre of Excellence for Climate Extremes, University of New South Wales, Sydney, Australia.

[2]Australian Centre for Excellence in Antarctic Science, University of New South Wales, Sydney, Australia.

[3]Research School of Earth Science and ARC Centre of Excellence for Climate Extremes, Australian National University, Canberra, Australia.

Contents of this file

1. Figures S1 to S9
2. Tables S1 to S4

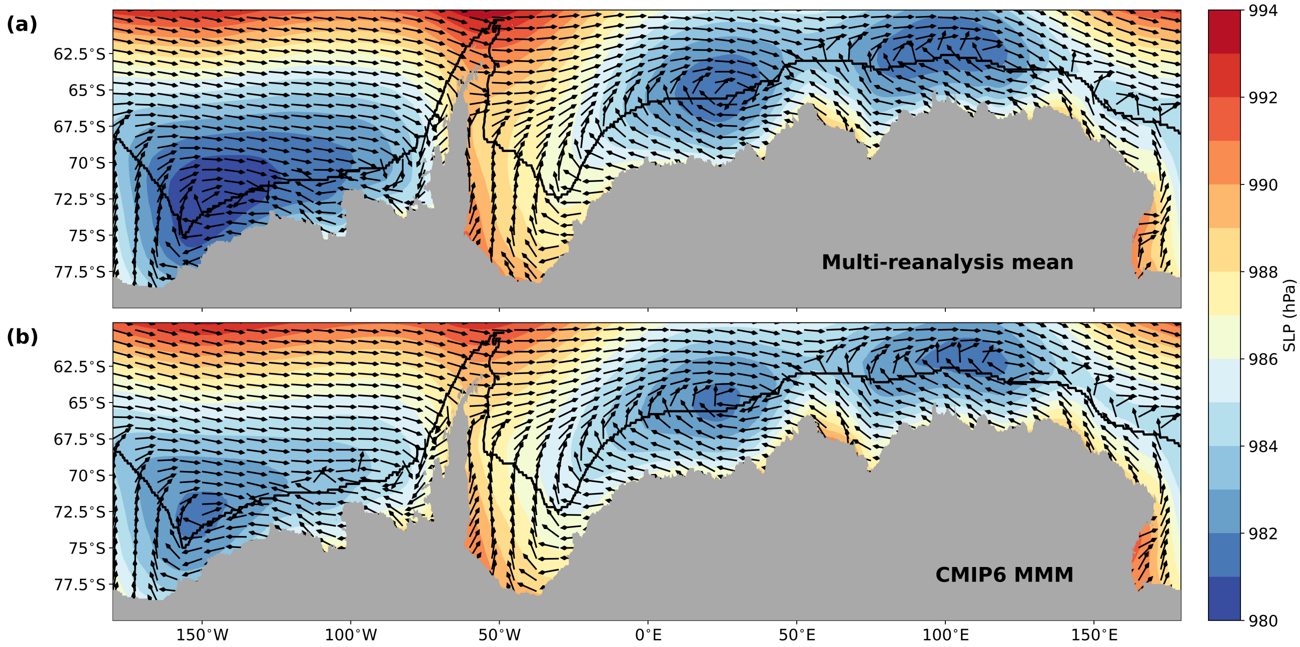

Figure S1. Sea level pressure and mean wind vectors for the historical period (1979 to 2015) of (a) the multi-reanalysis mean and (b) CMIP6 MMM. The black contour marks the northern limit of the study region.

Table S1. CMIP6 models included in the study

Model	Resolution & vertical levels	Modelling group	Reference
AWI-CM-1-1-MR	100km, L95.	Alfred Wegener Institute and Helmholtz Centre for Polar and Marine Research, Germany	(Semmler et al., 2020)
BCC-CSM2-MR	100km, L45	Beijing Climate Centre, China	(Wu et al., 2019)
CanESM5	500km, L49	Canadian Centre for Climate Modelling and Analysis, Environment and Climate Change Canada, Canada	(Swart et al., 2019)
EC-Earth3	100km, L91	European Community consortium, EU	
EC-Earth3-CC	100km, L91		
EC-Earth3-Veg	100km, L91		
EC-Earth3-Veg-LR	250km, L62		
FGOALS-f3-L	100km, L32	Institute of Atmospheric Physics, Chinese Academy of Sciences, China	(He et al., 2019)
GFDL-CM4	100km, L33	National Oceanic and Atmospheric Administration, Geophysical Fluid Dynamics Laboratory, USA	(Held et al., 2019)
GFDL-ESM4	100km, L49		(Krasting et al., 2018)
IITM-ESM	250km, L64	Centre for Climate Change Research, Indian Institute of Tropical Meteorology, India	(Krishnan et al., 2019)
INM-CM4-8	100km, L21	Institute for Numerical Mathematics, Russian Academy of Science, Russia	(E. M. Volodin et al., 2018)
INM-CM5-0	100km, L73	Institute for Numerical Mathematics, Russian Academy of Science, Russia	(E. Volodin & Gritsun, 2018)
IPSL-CM6A-LR	250km, L79	Institut Pierre Simon Laplace, France	(Boucher et al., 2020)
KACE-1-0-G	250km, L85	National Institute of Meteorological Sciences/Korea Meteorological Administration, Climate Research Division, Republic of Korea	(Lee et al., 2020)
MIROC6	250km, L81	JAMSTEC (Japan Agency for Marine-Earth Science and Technology, Japan), AORI (Atmosphere and Ocean Research Institute, The University of Tokyo, Japan), NIES (National Institute for Environmental Studies, Japan), and R-CCS (RIKEN Centre for Computational Science, Japan)	(Tatebe et al., 2019)
MPI-ESM1-2-LR	250km, L47		(Mauritsen et al., 2019)
MRI-ESM2-0	100km, L80	Meteorological Research Institute, Japan	(Yukimoto et al., 2011)
NESM3	250km, L47	Nanjing University of Information Science and Technology, China	(Cao et al., 2018)

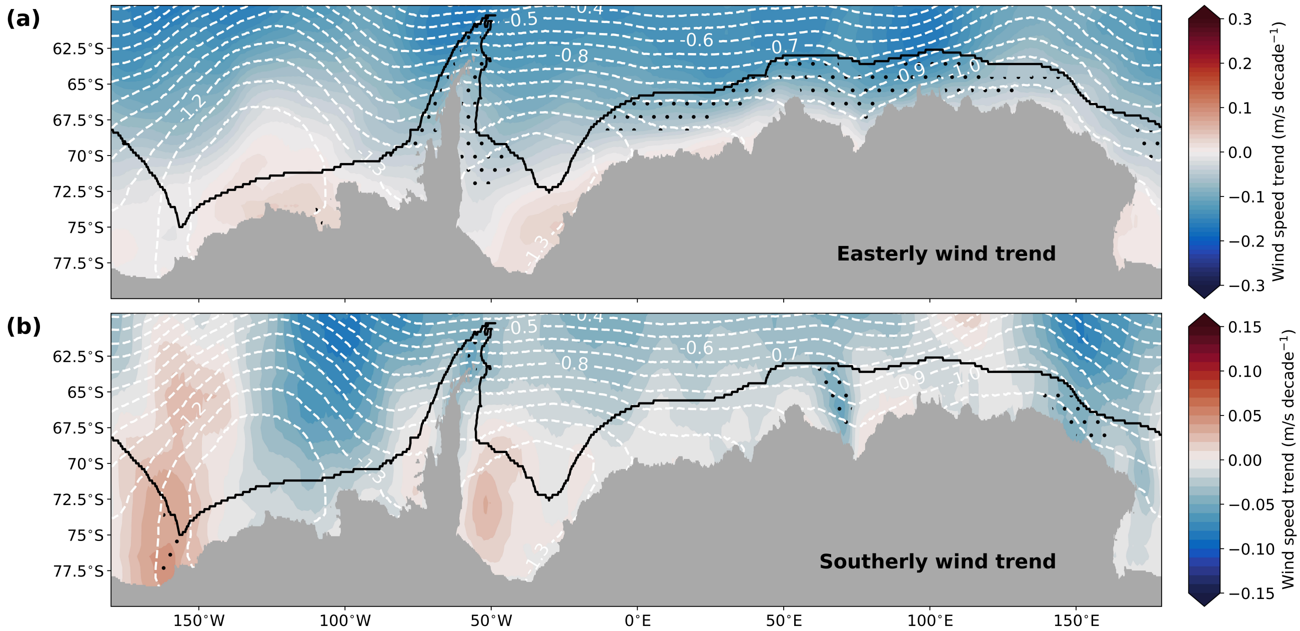

Figure S2. CMIP6 multimodel mean trends for (a) easterly and (b) southerly wind components for the historical period (1979 to 2015) with statistically significant trends ($p < 0.05$) hatched within the study region, south of the black contour. White contours show the sea level pressure difference of last ten years (2005 - 2015) with respect to the first ten years (1979 - 1989).

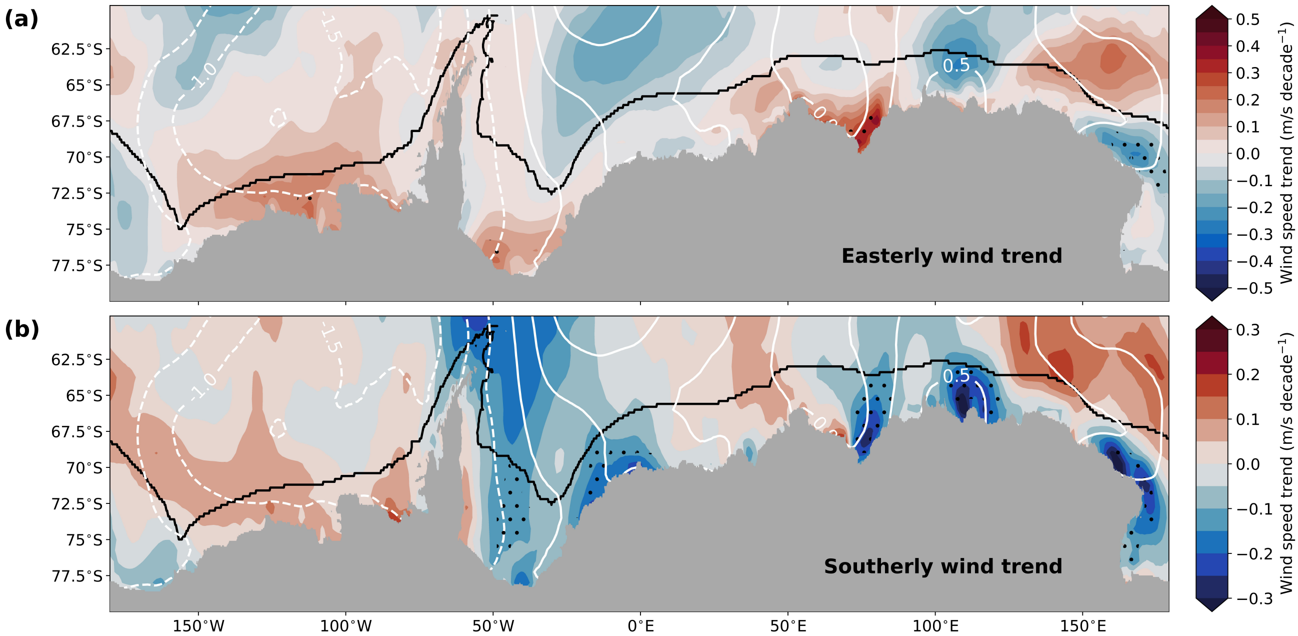

Figure S3. Multi-reanalysis mean trends for (a) easterly and (b) southerly wind components for the historical period (2015 to 2100) with statistically significant trends ($p < 0.05$) hatched within the study region, south of the black contour. White contours show the sea level pressure difference of last ten years (2005 - 2015) with respect to the first ten years (1979 - 1989).

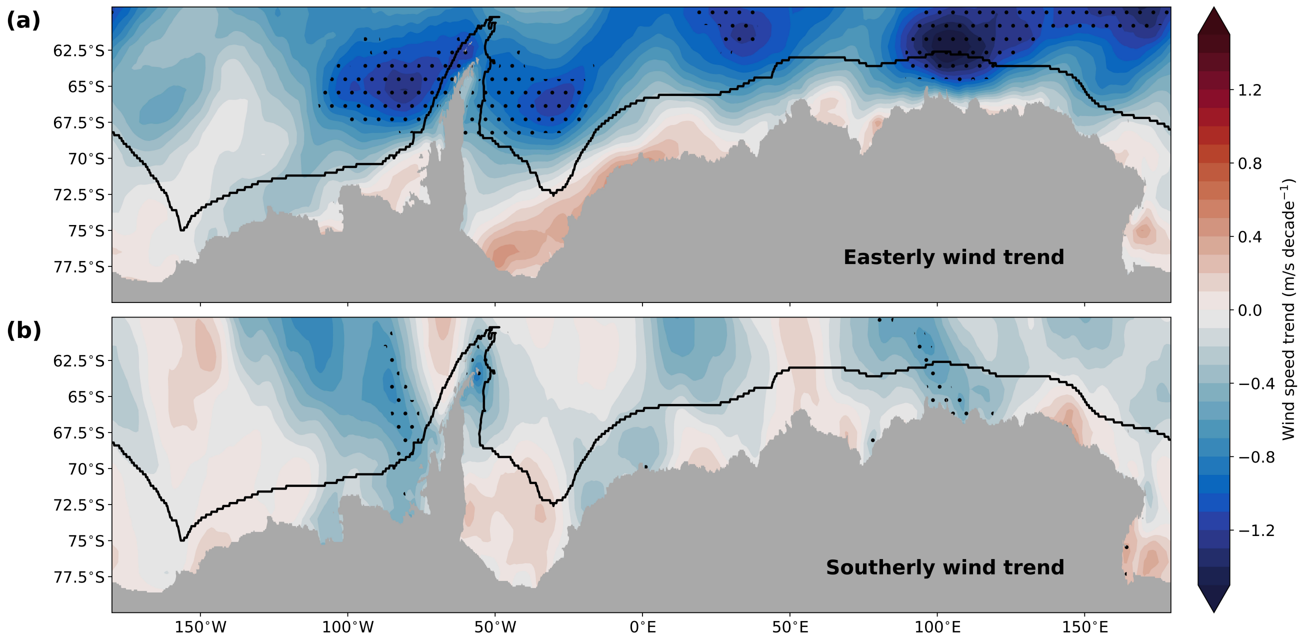

Figure S4. Multi-reanalysis summer (DJF) trends for (a) easterly and (b) southerly wind components for the period 1979 to 2000 with statistically significant trends ($p < 0.05$) hatched.

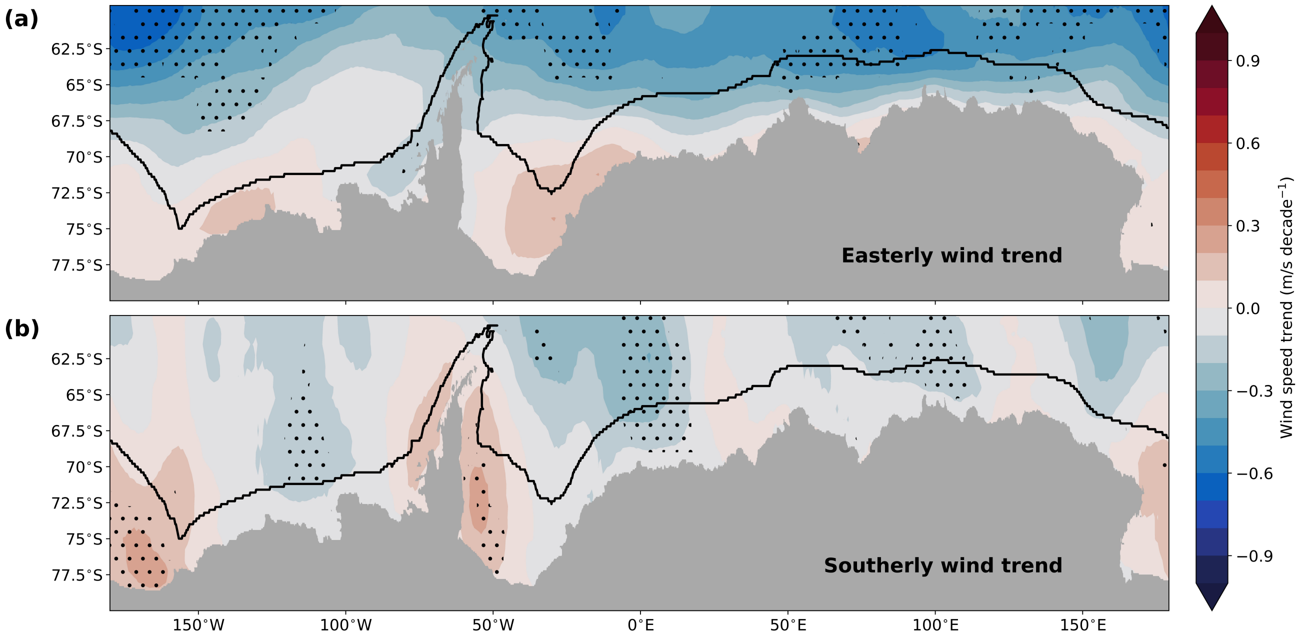

Figure S5. CMIP6 MMM summer (DJF) trends for (a) easterly and (b) southerly wind components for the period 1979 to 2000 with statistically significant trends ($p < 0.05$) hatched.

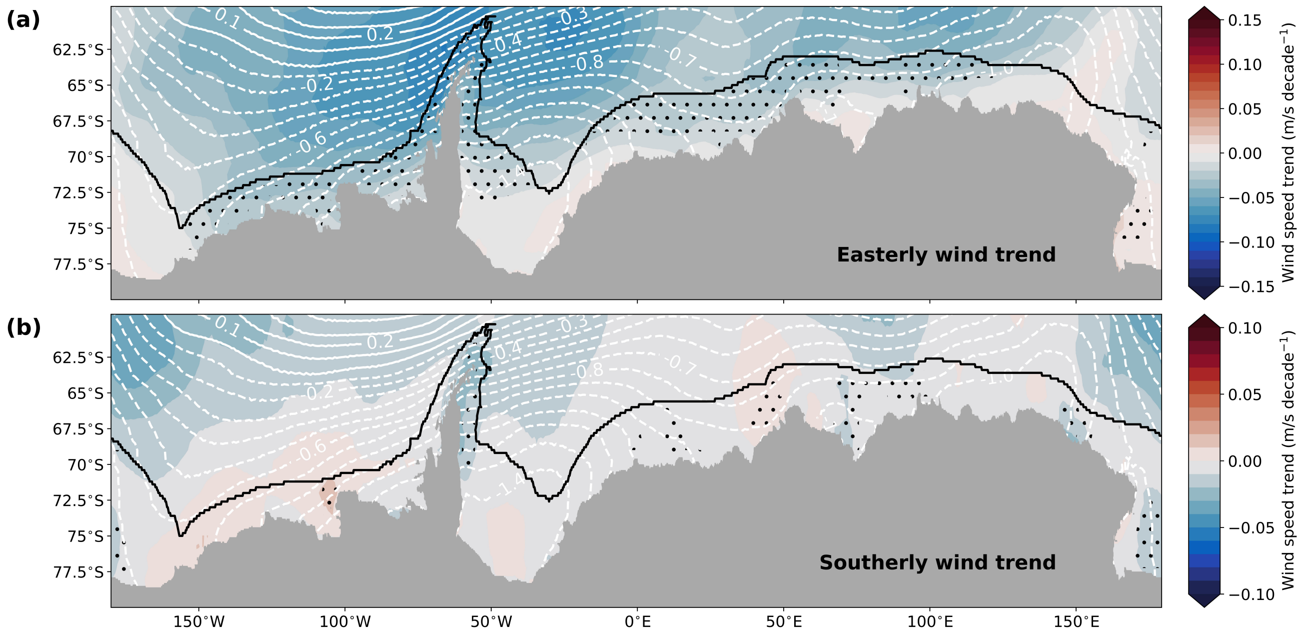

Figure S6. CMIP6 multi-model mean trends for a) easterly and b) southerly wind for emission scenario SSP245 during the period 2015 to 2100, with statistically significant trends with $p < 0.05$ hatched only for the study region. Pink contours show the difference in SLP of the last ten years (2090 to 2099) relative to the first ten years (2015 to 2025) and the black contour marks the northern limit of our study region.

Table S2. Easterly and southerly wind component trends (m/s century^{-1}) for individual reanalysis products, multi-reanalysis mean and CMIP6 MMM during the historical period and future projections under the SSP245 and SSP585 scenarios. Significant trends at 5% confident levels are highlighted in bold.

	Easterly wind trend	Southerly wind trend
Era-Interim	0.34	-0.03
ERA5	0.64	-0.004
CFSR	-0.06	**-0.84**
JRA55	-0.45	**-1.01**
Multi-reanalysis mean	0.11	**-0.47**
CMIP6 MMM Historical	**-0.41**	**-0.08**
CMIP6 MMM SSP245	**-0.17**	**-0.04**
CMIP6 MMM SSP585	**-0.56**	**-0.15**

Table S3. Easterly and southerly wind component trends (m/s century^{-1}) for the summer season (DJF) for individual reanalysis products, multi-reanalysis mean and CMIP6 MMM during the historical period and future projections under the SSP245 and SSP585 scenarios. Significant trends at 5% confident levels are highlighted in bold.

	Easterly wind trend	Southerly wind trend
Era-Interim	-1.17	-0.34
ERA5	0.74	-0.36
CFSR	-1.92	**-1.10**
JRA55	-1.04	**-0.83**
Multi-reanalysis mean	-1.22	**-0.65**
CMIP6 MMM Historical	**-1.08**	**-0.27**
CMIP6 MMM SSP245	**-0.24**	**-0.08**
CMIP6 MMM SSP585	**-0.84**	**-0.28**

Table S4. Easterly and southerly wind component trends (m/s century^{-1}) for the summer season (JJA) for individual reanalysis products, multi-reanalysis mean and CMIP6 MMM during the historical period and future projections under the SSP245 and SSP585 scenarios. Significant trends at 5% confident levels are highlighted in bold.

	Easterly wind trend	Southerly wind trend
Era-Interim	0.64	0.22
ERA5	0.94	0.27
CFSR	0.72	0.70
JRA55	-0.60	-1.07
Multi-reanalysis mean	0.43	-0.32
CMIP6 MMM Historical	0.32	0.08
CMIP6 MMM SSP245	-0.13	0.02
CMIP6 MMM SSP585	**-0.38**	-0.006

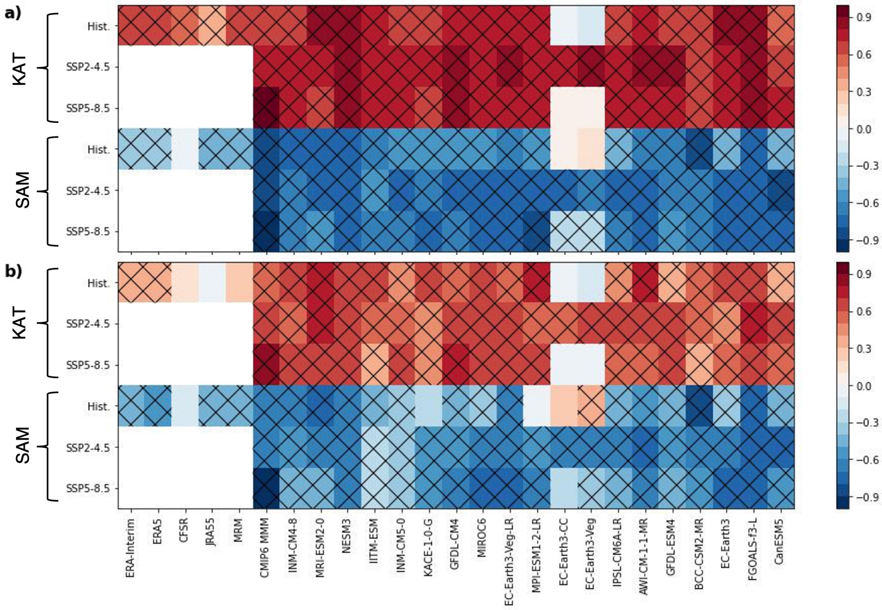

Figure S7. Correlations between the circumpolar average of the easterly and southerly wind components within the study region (time series in Figure 4) and the SAM and katabatic wind (KAT) indices for the (a) easterly and (b) southerly wind components during the historical period and future projections under SSP245 and SSP585 scenerios. Statistically significant correlations ($p < 0.05$) are hatched.

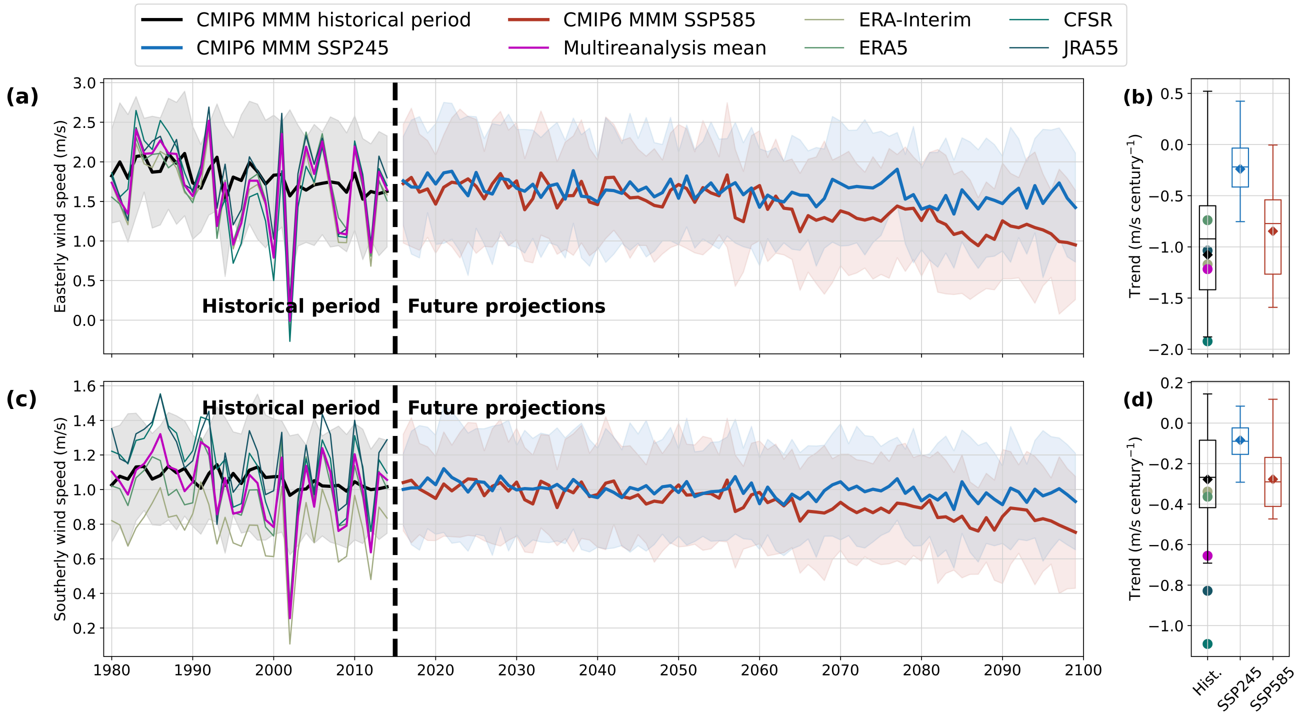

Figure S8. Summer time (December to February) (a) Easterly and (c) southerly wind speed averaged over the study region for CMIP6 multi-model mean and $\pm 1SD$ shading, the multi-reanalysis mean, ERA-Interim, ERA5, CFSR and JRA55. Boxplot of (b) easterly and (d) southerly wind trends (m/s decade^{-1}) for CMIP6 models for the historical period, SSP245 and SSP585. Dots mark trends in CMIP6 multi-model mean, multi-reanalysis mean, ERA-Interim, ERA5, CFSR and JRA55.

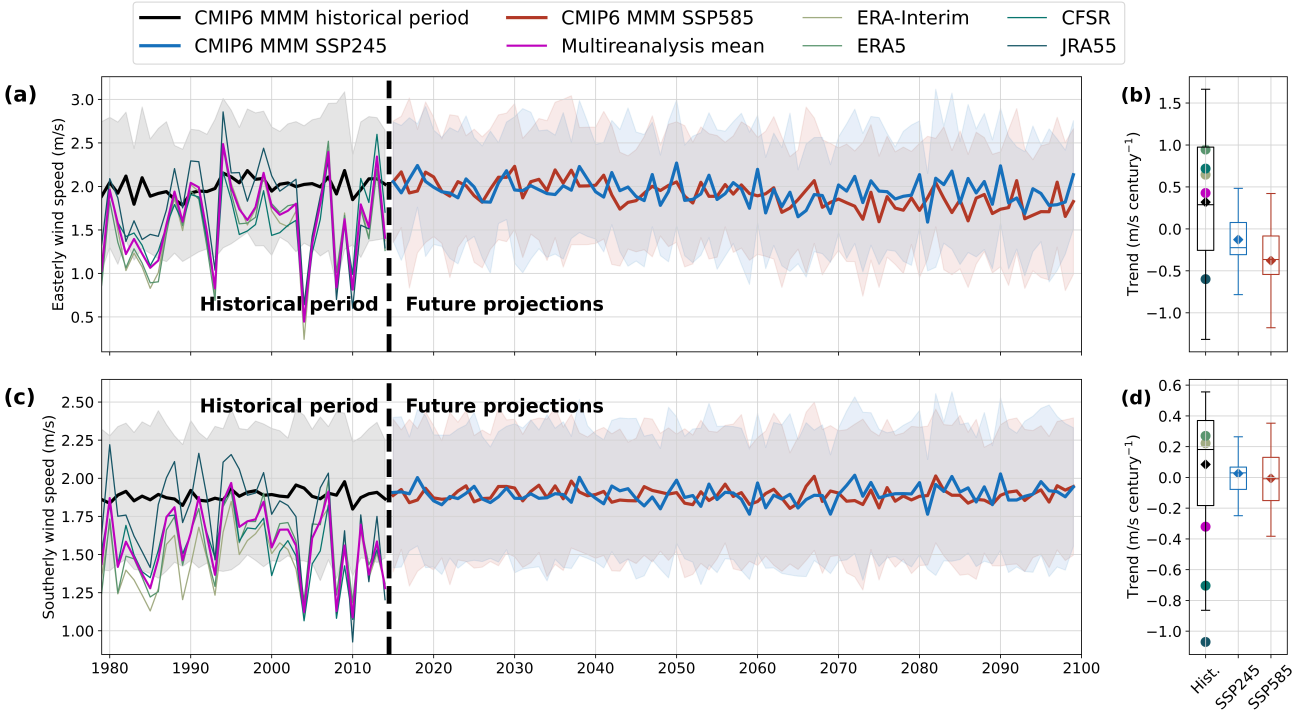

Figure S9. As in Figure S8 only shown for winter time (June to August).

References

Boucher, O., Servonnat, J., Albright, A. L., Aumont, O., Balkanski, Y., Bastrikov, V., . . . others (2020). Presentation and evaluation of the ipsl-cm6a-lr climate model. *Journal of Advances in Modeling Earth Systems*, *12*(7), e2019MS002010.

Cao, J., Wang, B., Yang, Y.-M., Ma, L., Li, J., Sun, B., . . . Wu, L. (2018). The nuist earth system model (nesm) version 3: description and preliminary evaluation. *Geoscientific Model Development*, *11*(7), 2975–2993.

He, B., Bao, Q., Wang, X., Zhou, L., Wu, X., Liu, Y., . . . others (2019). Cas fgoals-f3-l model datasets for cmip6 historical atmospheric model intercomparison project simulation. *Advances in Atmospheric Sciences*, *36*(8), 771–778.

Held, I., Guo, H., Adcroft, A., Dunne, J., Horowitz, L., Krasting, J., . . . others (2019). Structure and performance of gfdl's cm4. 0 climate model. *Journal of Advances in Modeling Earth Systems*, *11*(11), 3691–3727.

Krasting, J. P., John, J. G., Blanton, C., McHugh, C., Nikonov, S., Radhakrishnan, A., . . . others (2018). Noaa-gfdl gfdl-esm4 model output prepared for cmip6 cmip historical. *URL: https://doi. org/10.22033/ESGF/CMIP6*, *8597*.

Krishnan, R., Swapna, P., Vellore, R., Narayanasetti, S., Prajeesh, A., Choudhury, A. D., . . . Sanjay, J. (2019). The iitm earth system model (esm): development and future roadmap. In *Current trends in the representation of physical processes in weather and climate models* (pp. 183–195). Springer.

Lee, J., Kim, J., Sun, M.-A., Kim, B.-H., Moon, H., Sung, H. M., . . . Byun, Y.-H. (2020). Evaluation of the korea meteorological administration advanced community earth-system model (k-ace). *Asia-Pacific Journal of Atmospheric Sciences*, *56*(3), 381–395.

Mauritsen, T., Bader, J., Becker, T., Behrens, J., Bittner, M., Brokopf, R., ... others (2019). Developments in the mpi-m earth system model version 1.2 (mpi-esm1. 2) and its response to increasing co2. *Journal of Advances in Modeling Earth Systems*, *11*(4), 998–1038.

Semmler, T., Danilov, S., Gierz, P., Goessling, H. F., Hegewald, J., Hinrichs, C., ... others (2020). Simulations for cmip6 with the awi climate model awi-cm-1-1. *Journal of Advances in Modeling Earth Systems*, *12*(9), e2019MS002009.

Swart, N. C., Cole, J. N., Kharin, V. V., Lazare, M., Scinocca, J. F., Gillett, N. P., ... others (2019). The canadian earth system model version 5 (canesm5. 0.3). *Geoscientific Model Development*, *12*(11), 4823–4873.

Tatebe, H., Ogura, T., Nitta, T., Komuro, Y., Ogochi, K., Takemura, T., ... others (2019). Description and basic evaluation of simulated mean state, internal variability, and climate sensitivity in miroc6. *Geoscientific Model Development*, *12*(7), 2727–2765.

Volodin, E., & Gritsun, A. (2018). Simulation of observed climate changes in 1850–2014 with climate model inm-cm5. *Earth System Dynamics*, *9*(4), 1235–1242.

Volodin, E. M., Mortikov, E. V., Kostrykin, S. V., Galin, V. Y., Lykossov, V. N., Gritsun, A. S., ... others (2018). Simulation of the modern climate using the inm-cm48 climate model. *Russian Journal of Numerical Analysis and Mathematical Modelling*, *33*(6), 367–374.

Wu, T., Lu, Y., Fang, Y., Xin, X., Li, L., Li, W., ... others (2019). The beijing climate center climate system model (bcc-csm): The main progress from cmip5 to cmip6. *Geoscientific Model Development*, *12*(4), 1573–1600.

Yukimoto, S., Yoshimura, H., Hosaka, M., Sakami, T., Tsujino, H., HIRABARA, M., ... others

(2011). Meteorological research institute-earth system model version 1 (mri-esm1)-model description. (64), 92.